Liquid Crystals
Publication details, including instructions for authors and subscription information:
http://www.informaworld.com/smpp/title~content=t713926090

Thermotropic liquid crystals from a monosubstituted 2,2'-bipyridine

A. El-Ghayoury[a]; L. Douce[a]; R. Ziessel[a]; A. Skoulios[b]
[a] Laboratoire de Chimie, d'Electronique et de Photonique Moléculaires, ECPM/UPRES-A 7008 CNRS, 25 rue Becquerel, 67087 Strasbourg Cedex 2, France, [b] Groupe des Matériaux Organiques, IPCMS, URM 46, 23 rue du Loess, 67037 Strasbourg Cedex, France,

Online publication date: 06 August 2010

To cite this Article El-Ghayoury, A. , Douce, L. , Ziessel, R. and Skoulios, A.(2000) 'Thermotropic liquid crystals from a monosubstituted 2,2'-bipyridine', Liquid Crystals, 27: 12, 1653 — 1662
To link to this Article: DOI: 10.1080/026782900750037220
URL: http://dx.doi.org/10.1080/026782900750037220

LIQUID CRYSTALS, 2000, VOL. 27, NO. 12, 1653–1662

Thermotropic liquid crystals from a monosubstituted 2,2′-bipyridine

A. EL-GHAYOURY, L. DOUCE*, R. ZIESSEL*

Laboratoire de Chimie, d'Electronique et de Photonique Moléculaires, ECPM/UPRES-A 7008 CNRS, 25 rue Becquerel, 67087 Strasbourg Cedex 2, France

and A. SKOULIOS*

Groupe des Matériaux Organiques, IPCMS, URM 46, 23 rue du Loess, 67037 Strasbourg Cedex, France

(*Received 3 April 2000; in final form 24 May 2000; accepted 9 June 2000*)

Unsymmetric functionalization of 5-bromo-2,2′-bipyridine and 5,5′-dibromo-2,2′-bipyridine with 4-*n*-alkoxyphenylethynyl leads to two new families of mesomorphic compounds. The smectic B, smectic A and nematic phases observed were studied by polarizing optical microscopy, differential scanning calorimetry and X-ray diffraction. The structural parameters of the smectic phases were determined. The internal structure of the smectic phases, particularly the range of the in-layer ordering of the molecules, was investigated as a function of temperature.

1. Introduction

Oligopyridine frameworks (bipyridine, phenanthroline, terpyridine…) are well known in coordination chemistry to be powerful ligands towards almost any transition metal in different oxidation states [1]. These ligands are ideally suited for the construction of luminescent complexes and in the design of new optoelectronic devices [2, 3]. On the other hand, metal-containing liquid crystals have recently attracted considerable attention for their potential optical and magnetic properties and there is some hope of manufacturing these new materials into useful devices [4]. Over the last few years, a few examples of symmetrical polyimine-based liquid crystalline ligands and metallomesogens have been reported in the literature [5–7]. Surprisingly, only two examples of unsymmetrical ligands have, to our best knowledge, been reported in the literature; mesogenic by themselves [8], these proved however incapable of producing liquid crystals after complexation with a variety of transition metals (Pd, Fe, Mn, Mo…). To fill this gap, we thought it of interest to synthesize additional unsymmetrical ligands with a view to testing their ability to form liquid crystals firstly by themselves and eventually after complexation. In the light of the remarkable coordination and electronic properties of the bipyridine subunit, it is tempting to conclude that, at least in the future, unsymmetrical scafffoldings will not only prove to be capable of performing new functions on a molecular level, but will also have the ability to form rationally designed nanoscopic structures of predefined and predictable shapes and sizes [9].

The present paper deals with the synthesis of two homologous series of unsymmetrical bipyridine ligands and the study of their mesomorphic behaviour in the pure state. The compounds considered are 5-(4-alkyloxyphenylethynyl)-2,2′-bipyridine (abbreviated to *n*-ROPE-H, **4a–f**) and 5-bromo,5′-(4-alkyloxyphenylethynyl)-2,2′-bipyridine (abbreviated to *n*-ROPE-Br, **5a–f**).

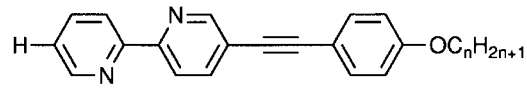

n-ROPE-H

4a : n = 6
4b : n = 8
4c : n = 10
4d : n = 12
4e : n = 14
4f : n = 16

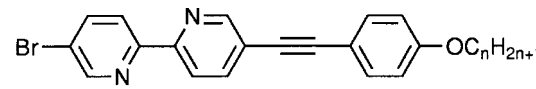

n-ROPE-Br

5a : n = 6
5b : n = 8
5c : n = 10
5d : n = 12
5e : n = 14
5f : n = 16

*Authors for correspondence; e-mail: ziessel@chimie.u-strasbg.fr

Liquid Crystals ISSN 0267-8292 print/ISSN 1366-5855 online © 2000 Taylor & Francis Ltd
http://www.tandf.co.uk/journals

2. Synthesis and characterization

The *n*-ROPE-H (**4a–f**) and *n*-ROPE-Br (**5a–f**) compounds were synthesized by Pd(0)-catalysed cross-coupling between 5-bromo-2,2′-bipyridine (**1**) or 5,5′-dibromo-2,2′-bipyridine (**3**) and 4-*n*-alkyloxypheny lacetylene (**2a–f**), according to schemes 1 and 2. The starting compounds **1**, **3** and **2a–f** were prepared as described in the literature [10, 11].

The compounds **4a–f** were prepared in excellent yields (*c.* 90% after purification) using a slight excess of **2a–f** with respect to **1**. During the synthesis of the **5a–f** compounds, care was taken to avoid double cross-coupling reactions by using stoichiometric amounts of reagents and lower concentrations of the Pd(0) catalyst; yields were then rather modest (*c.* 35% after purification). All compounds synthesized were characterized by elemental analysis, IR, ^{1}H, $^{13}C\{^{1}H\}$ NMR, and FAB-MS. Their purity was shown to be over 99%. The presence of an unsymmetrical ethynyl bridging group was confirmed by the presence of two signals in the $^{13}C\{^{1}H\}$ NMR in the range 85–94 ppm and one absorption peak around 2210 cm^{-1} in the IR spectra. All spectroscopic data are in keeping with the proposed molecular structures.

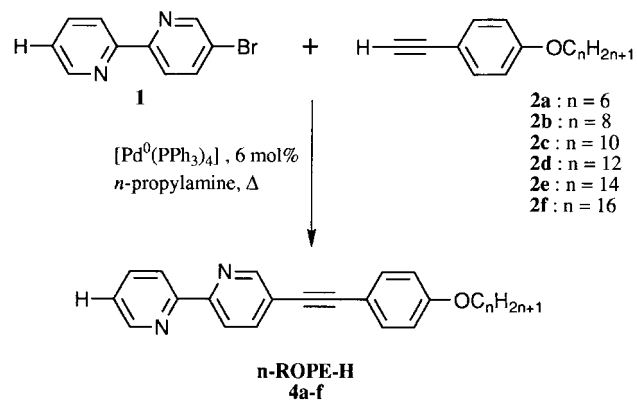

Scheme 1.

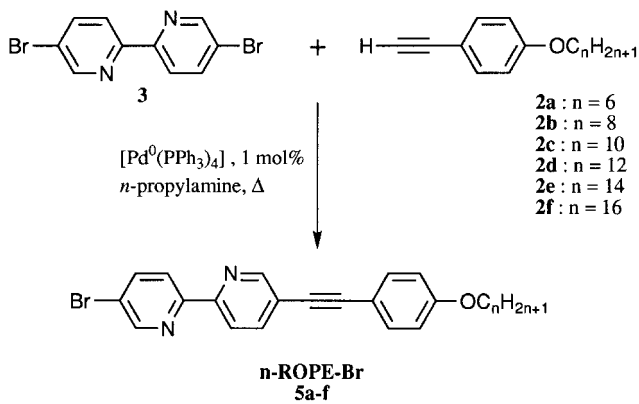

Scheme 2.

3. Results and discussion

The thermotropic liquid crystalline behaviour of the *n*-ROPE-H and *n*-ROPE-Br compounds was investigated using differential scanning calorimetry (Perkin-Elmer DSC7, heating and cooling rates of 5 K min^{-1}), polarizing optical microscopy (Leitz-Orthoplan, Mettler FP82 hot stage) and X-ray diffraction (XRD) (Guinier focusing camera, $CuK_{\alpha 1}$ radiation, powder samples in Lindemann capillaries, INSTEC hot stage, INEL CPS-120 curved position-sensitive detector). For the sake of simplicity, the results obtained are immediately summarized in figures 1 and 2.

The DSC thermograms, registered upon heating and subsequent cooling, showed the presence of sharp peaks

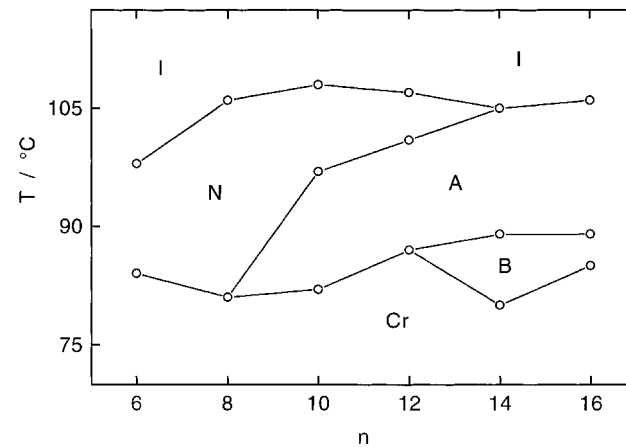

Figure 1. Transition temperatures of the *n*-ROPE-H compounds as a function of the number of carbon atoms in the alkyl chains (I = isotropic liquid, N = nematic phase, A = smectic A phase, B = smectic B phase, Cr = crystal phase).

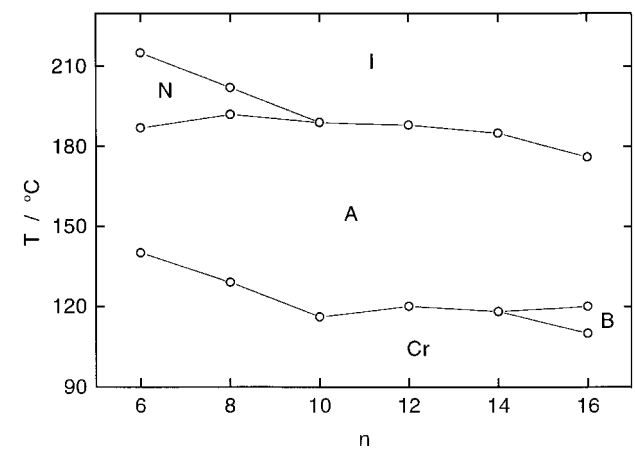

Figure 2. Transition temperatures of the *n*-ROPE-Br compounds as a function of the number of carbon atoms in the alkyl chains (I = isotropic liquid, N = nematic phase, A = smectic A phase, B = smectic B phase, Cr = crystal phase).

indicative of first order phase transitions. Corresponding to the disordering of the alkyl chains, the melting of the crystal into a nematic, a smectic A or a smectic B phase involves a significant enthalpy change ranging from about 40 to 90 J g^{-1}. The reverse transition, induced by cooling, takes place with a strong hysteresis of about 10 to 30°C. For *n*-ROPE-H ($n \leqslant 12$) and *n*-ROPE-Br ($n \leqslant 14$), apart from the $n = 6$ derivatives, this transition proceeds through an additional monotropic smectic B phase. The other transitions, occurring between two liquid crystal phases or between a liquid crystal and the isotropic liquid, take place with hardly any hysteresis and involve rather small enthalpy changes: ~2 J g^{-1} for nematic to isotropic, ~4 J g^{-1} for smectic A to nematic, ~3 J g^{-1} for smectic B to smectic A, and ~15 J g^{-1} for smectic A to isotropic. The transition temperatures of the compounds ROPE-H and ROPE-Br are gathered in tables 1 and 2.

The optical textures observed upon slow cooling from the isotropic melt clearly showed the existence of the phases mentioned above (figures 1 and 2). The formation of the nematic phases was indicated by the appearance of birefringent droplets coalescing to form two- and four-brush schlieren textures (rapidly transforming for 6-ROPE-Br and 8-ROPE-Br into a threaded texture). The formation of the smectic A phases was attested by the appearance of bâtonnets merging into wide fan-like, focal-conic textures. In the particular case of 16-ROPE-H, the isotropic to smectic A phase transition involves a transient nematic phase. Both schlieren and focal-conic textures form and evolve steadily into homeotropy, thus revealing the uniaxial character of the phases involved. The transformation of smectic A into smectic B was easily detected by the appearance of mosaic textures for *n*-ROPE-H and of faintly striated focal-conic textures for *n*-ROPE-Br. The uniaxial character of the smectic B was ascertained by encouraging homeotropy using glass plates treated with octadecyltrichlo rosilane. The formation of smectic A starting from a homeotropic nematic phase is revealed by the emergence of narrow focal-conic fringes between wide homeotropic domains.

Table 1. Phase transitions (°C) of the *n*-ROPE-H compounds **4a–f** (I = isotropic liquid, N = nematic phase, A = smectic A phase, B = smectic B phase, Cr = crystal phase).

Compound	Transitions
4a; $n = 6$	Cr $\xrightarrow{84}$ N $\underset{}{\overset{98}{\longleftrightarrow}}$ I
4b; $n = 8$	Cr $\xrightarrow{81}$ N $\underset{}{\overset{106}{\longleftrightarrow}}$ I
4c; $n = 10$	Cr $\xrightarrow{82}$ A $\underset{}{\overset{97}{\longleftrightarrow}}$ N $\underset{}{\overset{108}{\longleftrightarrow}}$ I
4d; $n = 12$	Cr $\xrightarrow{87}$ A $\underset{}{\overset{101}{\longleftrightarrow}}$ N $\underset{}{\overset{107}{\longleftrightarrow}}$ I
4e; $n = 14$	Cr $\xrightarrow{80}$ B $\underset{}{\overset{89}{\longleftrightarrow}}$ A $\underset{}{\overset{105}{\longleftrightarrow}}$ I
4f; $n = 16$	Cr $\xrightarrow{85}$ B $\underset{}{\overset{89}{\longleftrightarrow}}$ A $\underset{}{\overset{106}{\longleftrightarrow}}$ I

Table 2. Phase transitions (°C) of the *n*-ROPE-Br compounds **5a–f** (I = isotropic liquid, N = nematic phase, A = smectic A phase, B = smectic B phase, Cr = crystal phase).

Compound	Transitions
5a; $n = 6$	Cr $\xrightarrow{140}$ A $\underset{}{\overset{187}{\longleftrightarrow}}$ N $\underset{}{\overset{215}{\longleftrightarrow}}$ I
5b; $n = 8$	Cr $\xrightarrow{129}$ A $\underset{}{\overset{192}{\longleftrightarrow}}$ N $\underset{}{\overset{202}{\longleftrightarrow}}$ I
5c; $n = 10$	Cr $\xrightarrow{116}$ A $\underset{}{\overset{189}{\longleftrightarrow}}$ I
5d; $n = 12$	Cr $\xrightarrow{120}$ A $\underset{}{\overset{188}{\longleftrightarrow}}$ I
5e; $n = 14$	Cr $\xrightarrow{118}$ A $\underset{}{\overset{185}{\longleftrightarrow}}$ I
5f; $n = 16$	Cr $\xrightarrow{110}$ B $\underset{}{\overset{120}{\longleftrightarrow}}$ A $\underset{}{\overset{176}{\longleftrightarrow}}$ I

The structures of all the liquid crystal phases were definitely established using (XRD). The smectic A structure was characterized by patterns containing one or two sharp, equidistant reflections in the small angle region, related to the smectic layering, and a broad band in the wide angle region, related both to the disordered conformation of the alkyl chains and the liquid-like lateral correlations of the aromatic cores within the layers; see figure 3 (*a*). The smectic B structure was characterized by patterns containing an additional narrow band in the wide angle region, related to the hexagonal lateral packing of the aromatic cores inside the layers; see figure 3 (*b*). Finally, the nematic phase was characterized by X-ray patterns devoid of sharp reflections, in which the broad small angle band is related to the presence of cybotactic fluctuations; see figure 3 (*c*).

Measured from the angular position of the sharp small angle reflections, the spacings of the smectic A and smectic B phases were found to be virtually independent of temperature, their relative thermal expansion coefficient being only $(\partial d/\partial T)/d \approx +3 \times 10^{-4}\,K^{-1}$ and unsignificant for all practical purposes. The spacings did not change perceptibly at the transition from smectic B to smectic A (figure 4), indicating that the structures of the two phases are globally similar and of the well known single layered smectic type, in which the spacings found compare well with the length of the molecules in an all-*trans* fully extended conformation (estimated by molecular modelling, using PC Spartan Plus software) (figures 5 and 6). Standing upright in a head to tail interdigitated configuration, the aromatic cores of the molecules are arranged in single layers separated by the alkyl chains in a disordered conformation (figure 7). It is fair to note that, strictly speaking, the smectic layers of the *n*-ROPE-Br derivatives slightly exceed the length of the molecules, by about 1 Å. Very likely, the small extra

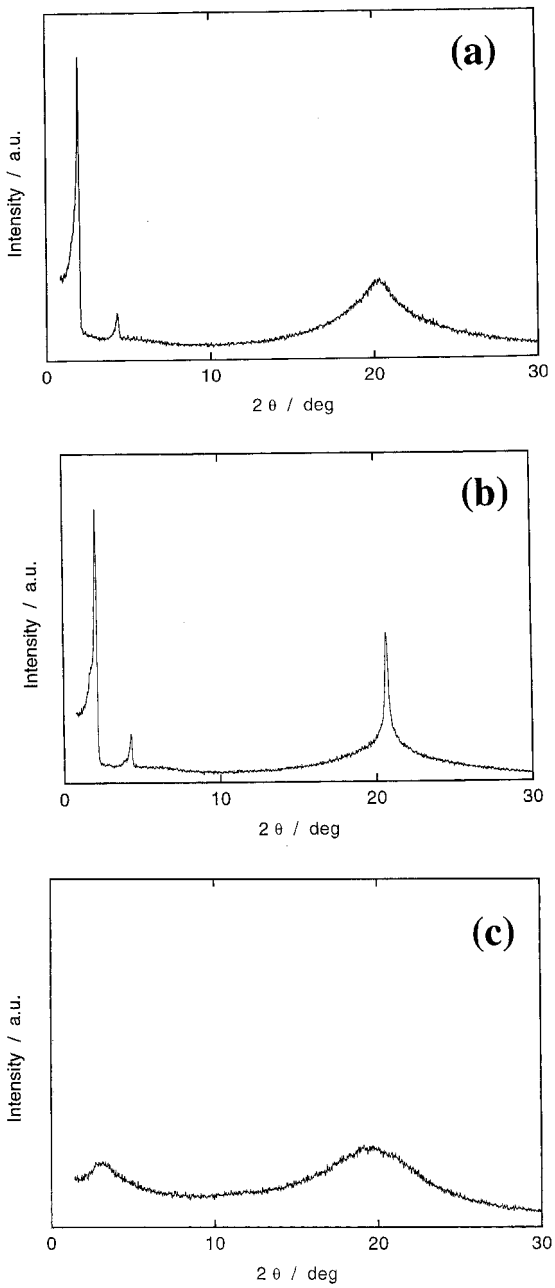

Figure 3. X-ray diffraction patterns (*a*) of 14-ROPE-Br in the smectic A state at 126°C, (*b*) of 16-ROPE-Br in the smectic B state at 110°C, and (*c*) of 8-ROPE-H in the nematic state at 97.5°C.

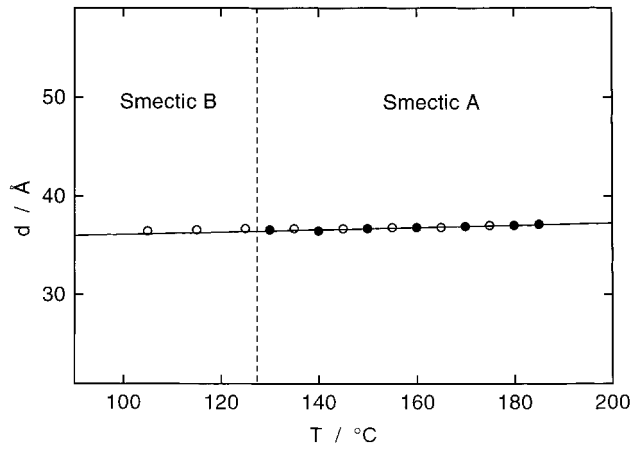

Figure 4. Temperature dependence of the smectic period of 12-ROPE-Br in the smectic A and smectic B states. Data were collected upon heating (solid circles) and subsequent cooling (open circles) of the samples.

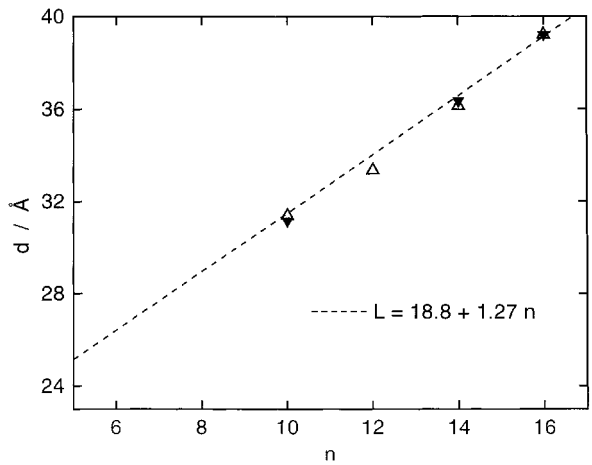

Figure 5. Variation of the smectic period of *n*-ROPE-H in the smectic A state at 95°C (open triangles) and smectic B state at 82°C (solid triangles) as a function of the number of carbon atoms in the alkyl chains. The dashed line represents the length of the molecules in a fully extended conformation, estimated by molecular modelling.

thickness originates in the fact that, owing to van der Waals interactions, the aromatic cores are slightly shifted along their axes to allow the highly polarizable bromines to bury themselves deeper inside the aromatic layers.

Corresponding with the size of the molecules, the smectic periods increase linearly with the number n of carbon atoms in the alkyl chains (figures 5 and 6), according to the equations: $d(\text{Å}) = 17.9_{\pm 1.2} + 1.32_{\pm 0.09}\, n$ for *n*-ROPE-H, and $d(\text{Å}) = 20.9_{\pm 0.8} + 1.33_{\pm 0.07}\, n$ for *n*-ROPE-Br (as deduced from a least squares linear fit of the experimental data). Analytically expressed by the equation $d = V/\sigma = (V_0 + nV_{CH2})/\sigma$ (where σ is the cross-sectional area of the aromatic cores, while V, V_{CH2} and V_0 represent the respective volumes of one molecule, one methylene group and one molecule deprived of all its methylene groups), the linear behaviour of d versus n suggests that σ is indeed independent of n. From the slope of the corresponding straight lines and the known value of V_{CH2} at the appropriate temperature ($V_{CH_2} = 25.93 + 2.076 \times 10^{-2}\, \text{T(°C)}\,\text{Å}^3$ [12]), one may easily calculate [13] the cross-sectional area of the aromatic cores. The values found are: $21 \pm 1\,\text{Å}^2$ for *n*-ROPE-H in

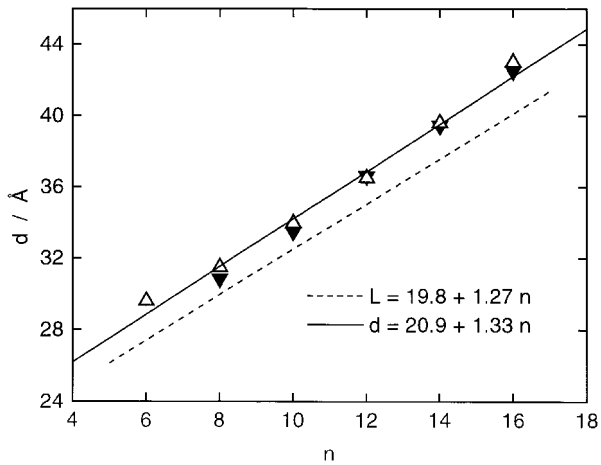

Figure 6. Variation of the smectic period of *n*-ROPE-Br in the smectic A state at 160°C (open triangles) and smectic B state at 120°C (solid triangles) as a function of the number of carbon atoms in the alkyl chains. The dashed straight line represents the length of the molecules in a fully extended conformation, estimated by molecular modelling. The solid straight line describes the *n*-dependence of the smectic periods as determined by a least squares linear fit of the experimental data.

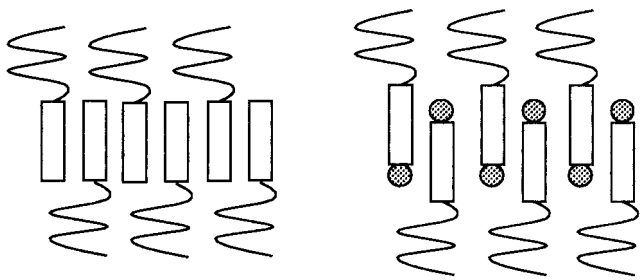

Figure 7. Schematic representation of the single-layered smectic A or B structure of *n*-ROPE-H (left) and *n*-ROPE-Br (right). For simplicity, the disordered alkyl chains are depicted by wavy lines, the aromatic cores by rectangles, and the bromo substituents by grey circles.

the smectic A state at 95°C and in the smectic B state at 82°C, 22 ± 1 Å^2 for the smectic A of *n*-ROPE-Br at 160°C, and 21 ± 1 Å^2 for the smectic B of *n*-ROPE-Br at 120°C. These values agree well with that (21.4 Å^2) determined for all the smectic B phases from the spacing (4.30 Å) of the sharp wide angle reflection.

In an attempt to get a deeper insight into the internal structure of the smectic layers and into the phase transitions observed from smectic B to smectic A, the profile of the wide angle X-ray scattering signals was analysed as a function of temperature. Normally, because of the three-dimensional extension of the signals in reciprocal space, such a study requires the use of well oriented samples and high-resolution X-ray techniques. As only powder patterns were available in the present work for practical reasons, our investigation was of necessity confined to a simple evaluation of the temperature dependence of the in-layer ordering of the molecules on a qualitative basis. A least squares double Lorentzian fit of the experimental data shows that the wide angle scattering of the smectic B and smectic A phases results from the superposition of two distinct rings, one diffuse ring related to the disordered conformation of the alkyl chains and one more or less narrow ring related to the hexagonal packing of the aromatic cores inside the smectic layers (figure 8). The width of the latter ring allows a rough estimate of the correlation length ξ of the in-plane positional ordering of the molecules to be made. Plotted as a function of temperature, the ξ value decays steadily with increasing temperature, falling

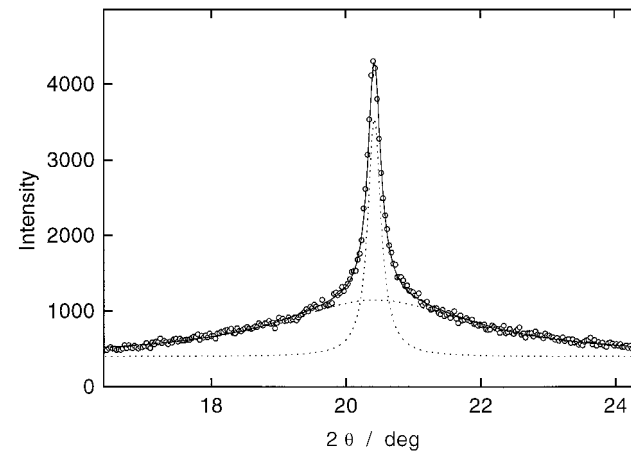

(*a*)

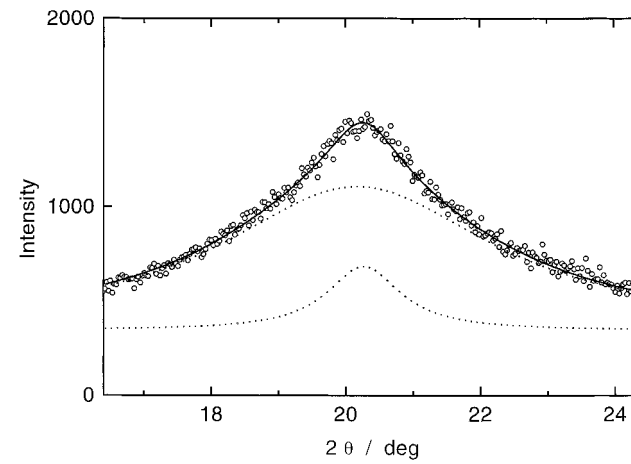

(*b*)

Figure 8. Profile of the X-ray scattering in the wide angle region of the diffraction patterns of 14-ROPE-Br (*a*) in the smectic B state at 110°C and (*b*) in the smectic A state at 128°C, as analysed by a least squares double-Lorentzian fit of the experimental data.

abruptly at the transition from smectic B to smectic A (figure 9). Apparently, ξ decreases in a linear fashion for smectic B from about 370 to 67 Å, while it decreases exponentially for smectic A from 30 to 20 Å. Whatever its theoretical basis, the disordering of the aromatic cores in the smectic B and smectic A phases increases practically continuously with temperature, except for a small jump at the first order phase transition from smectic B to smectic A; this is very weak as witnessed by the small enthalpy change involved.

According to theory, there are only two distinct types of B phase [14]. In crystal B, the layers superposed are two-dimensional crystals; owing to their (weak) interactions, they are positionally locked together to form a three-dimensional crystal. In hexatic B (a true smectic), the layers are two-dimensional hexatics, with short range positional and long range orientational correlations of the molecules; owing to their negligible positional interactions, they are free to slide on top of one another, but yet able to preserve a common orientation in three-dimensional space. In the present work, the existence of a three-dimensional crystal lattice is denied by the experimental evidence collected: absence of extra side reflections in the wide angle region—see figure 8 (*a*)—and dramatic widening with increasing temperature of the wide angle reflection from the in-layer ordering of the molecules. There is no other option, therefore, but to consider the B phases studied here as hexatic smectic B in nature, even though all attempts to reveal a characteristic six-fold modulation of the wide angle reflection, using the 'freely suspended thin film' technique [15], were totally unsuccessful.

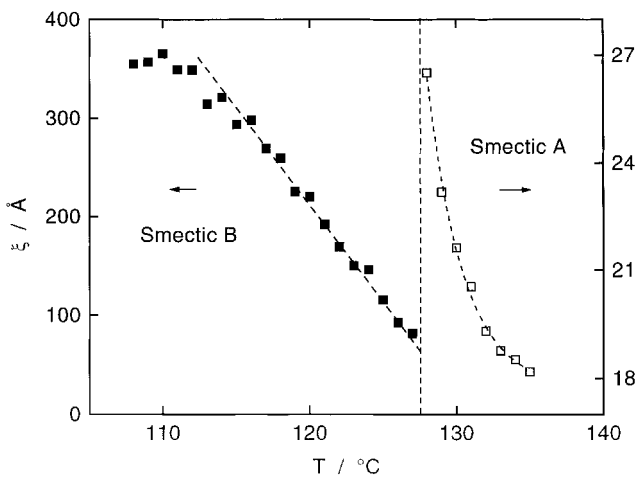

Figure 9. Temperature dependence of the correlation range of the in-plane hexagonal packing of the 14-ROPE-Br molecules in the smectic B and smectic A states, as estimated by the least squares double Lorentzian fit of the experimental data shown in figure 8.

4. Concluding remarks

In the present work, two series of unsymmetrical mesogenic compounds involving the 2,2′-bipyridine framework, were synthesized. In one of them, the molecules end in a bromo substituent which is available for future use in the synthesis of other novel mesogenic compounds designed to display properties that are deemed useful. In the other, the molecules have no terminal group, which is rare enough to be noted. It is of interest to add that, in this particular series the nematic phase is present for all the compounds investigated whatever the length of their alkyl chains. Finally, the range of the in-layer ordering of the molecules in the smectic B phases decreases considerably with increasing temperature, to reach values well below 100 Å near the smectic A phase.

5. Experimental

All reactions were carried out under argon in Schlenk-type flasks. The propylamine and di-isopropylamine used as solvents were distilled over KOH under argon. Infrared spectra were recorded in the region 4000–400 cm^{-1} using an FTIR Bruker IFS-66 spectrophotometer. ^1H (200.1 MHz) and $^{13}C\{^1H\}$ (50.3 MHz) NMR spectra were recorded at room temperature with a FT Bruker AC-200 instrument, using deuteriated chloroform as a solvent and internal standard: δ (H) are in ppm relative to residual protiated solvent (7.26) and δ (C) in ppm are relative to $CDCl_3$ (77.03). Fast atomic bombardment (FAB, positive mode) spectra were recorded using a ZAB-HF-VB-analytical apparatus and *m*-nitrobenzylalcohol (*m*-NBA).

5.1. *5-(4-Hexyloxyphenylethyny l)-2,2′-bipyridine (**4a**)*

5-Bromo-2,2′-bipyridine (0.20 g, 0.85 mmol), 1-ethynyl-4-hexyloxybenzene (**2a**) (0.207 g, 1.02 mmol), and $[Pd(PPh_3)_4]$ (0.030 g; 3 mol %) were dissolved in argon-degassed *n*-$PrNH_2$ (15 ml). The yellow solution was heated at 60°C for 3 days. After evaporation of the solvent, the residue was purified by flash chromatography (silica gel column, elution with a gradient of hexane/CH_2Cl_2: 95/5 to 40/60 v/v) and recrystallized from CH_2Cl_2/hexane. Yield: white powder (0.28 g, 93%). $R_f = 0.3$ (CCM, SiO_2, hexane/CH_2Cl_2, 50/50 v/v). ^1H NMR (200.1 MHz, $CDCl_3$, 25°C): $\delta = 8.79$ ppm (d, ^4J (H,H) = 1.5 Hz, 1H), 8.67 (broad d, J (H,H) = 4.0 Hz, in reality ddd corresponding to $^3J + {}^4J + {}^5J$, 1H), 8.41 (m, 2H), 7.89 (dd, ^3J (H,H) = 8.2 Hz, ^4J (H,H) = 2.1 Hz, 1H), 7.79 (dd, ^3J (H,H) = 7.8 Hz, ^4J (H,H) = 1.8 Hz, 1H), 7.28 (m, 1H), 7.17 (AB system, J (AB) = 8.9 Hz, $\Delta\nu$ = 123.0 Hz, 4H), 3.93 (t, ^3J (H,H) = 6.4 Hz, 2H, OCH_2), 1.77 (m, 2H, CH_2), 1.34 (m, 6H), 0.90 (t, ^3J (H,H) = 6.4 Hz, 3H, CH_3). ^{13}C $\{^1H\}$ NMR (50.3 MHz, $CDCl_3$, 25°C): $\delta = 159.55$, 155.43, 154.29, 151.35, 149.15, 139.00,

136.80, 133.42, 123.71, 121.18, 120.63, 120.18, 114.49, 114.27 (C-aromatics), 93.76 (C≡C), 85.01 (C≡C), 67.96 (OCH_2), 31.47 (CH_2), 29.04 (CH_2), 25.58 (CH_2), 22.50 (CH_2), 13.97 (CH_3). FTIR (KBr, ν/cm^{-1}): 2919 (s), 2859 (s), 2210 (m, $\nu_{C\equiv C}$), 1597 (s), 1575 (m), 1507 (s), 1459 (m), 1391 (w), 1287 (m), 1247 (s), 1111 (s), 1025 (m), 990 (w), 831 (w). FAB$^+$-MS (*m*-NBA): $[M + H]^+$ (% rel. int.): 357.6 (100). Elemental analysis, calc. (found) for $C_{24}H_{24}N_2O$ (M_r = 356.472): C 80.87 (80.73), H 6.79 (6.70), N 7.86 (7.80)%.

5.2. *5-(4-Octyloxyphenylethynyl)-2,2′-bipyridine (**4b**)*

Experimental procedure as for **4a**. Yield: white powder (0.29 g, 89%). R_f = 0.3 (CCM, SiO_2, hexane/CH_2Cl_2, 50/50, v/v). ^{1}H NMR (200.1 MHz, $CDCl_3$, 25°C): δ = 8.79 ppm (dd, ^4J (H,H) = 1.5 Hz, ^5J (H,H) = 0.6 Hz, 1H), 8.68 (m, 1H), 8.40 (m, 2H), 7.90 (dd, ^3J (H,H) = 8.2 Hz, ^4J (H,H) = 2.1 Hz, 1H), 7.81 (ddd, ^3J (H,H) = 7.8 Hz, ^4J (H,H) = 1.5 Hz, 1H), 7.30 (m, 1H), 7.19 (AB system, J (AB) = 8.9 Hz, $\Delta\nu$ = 122.1 Hz, 4H), 3.96 (t, ^3J (H,H) = 6.4 Hz, 2H, OCH_2), 1.79 (m, 2H, CH_2), 1.30 (m, 10H), 0.90 (t, ^3J (H,H) = 4.0 Hz, 3H, CH_3). ^{13}C {^{1}H} NMR (50.3 MHz, $CDCl_3$, 25°C): δ = 159.55, 155.47, 154.33, 151.35, 149.15, 139.00, 136.83, 133.12, 123.71, 121.18, 120.66, 120.22, 114.53, 114.27 (C-aromatics), 93.76 (C≡C), 85.01 (C≡C), 68.00 (OCH_2), 31.72 (CH_2), 29.26 (CH_2), 29.15 (CH_2), 29.10 (CH_2), 25.92 (CH_2), 22.57 (CH_2), 14.04 (CH_3). FTIR (KBr, ν/cm^{-1}): 2931 (s), 2859 (m), 2210 (w, $\nu_{C\equiv C}$), 1598 (m), 1575 (w), 1540 (w), 1508 (s), 1461 (s), 1371 (w), 1287 (m), 1251 (s), 1172 (w), 1112 (s), 1030 (w), 859 (w), 828 (m). FAB$^+$-MS (*m*-NBA): $[M + H]^+$ (% rel. int.): 385.1 (100). Elemental analysis, calc. (found) for $C_{26}H_{28}N_2O$ (M_r = 384.526): C 81.21 (80.90), H 7.34 (6.99), N 7.29 (6.96)%.

5.3. *5-(4-Decyloxyphenylethynyl)-2,2′-bipyridine (**4c**)*

Experimental procedure as for **4a**. Yield: white powder (0.33 g, 94%). R_f = 0.3 (CCM, SiO_2, hexane/CH_2Cl_2, 50/50, v/v). ^{1}H NMR (200.1 MHz, $CDCl_3$, 25°C): δ = 8.79 ppm (dd, ^4J (H,H) = 2.1 Hz, ^5J (H,H) = 0.9 Hz, 1H), 8.68 (m, 1H), 8.41 (m, 2H), 7.90 (dd, ^3J (H,H) = 8.2 Hz, ^4J (H,H) = 2.1 Hz, 1H), 7.81 (ddd, ^3J (H,H) = 7.8 Hz, ^4J (H,H) = 1.8 Hz, 1H), 7.30 (m, 1H), 7.19 (AB system, J (AB) = 9.0 Hz, $\Delta\nu$ = 121.1 Hz, 4H), 3.96 (t, ^3J (H,H) = 6.6 Hz, 2H, OCH_2), 1.79 (m, 2H, CH_2), 1.33 (*b*s, 14H), 0.89 (t, ^3J (H,H) = 6.4 Hz, 3H, CH_3). ^{13}C {^{1}H} NMR (50.3 MHz, $CDCl_3$, 25°C): δ = 159.55, 155.47, 154.33, 151.35, 149.15, 139.00, 136.83, 133.12, 123.71, 121.18, 120.66, 120.22, 114.53, 114.27 (C-aromatics), 93.72 (C≡C), 85.01 (C≡C), 68.00 (OCH_2), 31.83 (CH_2), 29.48 (CH_2), 29.30 (CH_2), 29.08 (CH_2), 25.92 (CH_2), 22.61 (CH_2), 14.04 (CH_2). FTIR (KBr, ν/cm^{-1}): 2920 (s), 2853 (m), 2209 (w, $\nu_{C\equiv C}$), 1606 (m), 1575 (w), 1511 (m), 1461 (m), 1294 (m), 1253 (s), 1111 (s), 1021 (w), 828 (m). FAB$^+$-MS (*m*-NBA): $[M + H]^+$ (% rel. int.): 413.2 (100). Elemental analysis, calc. (found) for $C_{28}H_{32}N_2O$ (M_r = 412.587): C 81.51 (81.37), H 7.82 (7.65), N 6.79 (6.69)%.

5.4. *5-(4-Dodecyloxyphenylethynyl)-2,2′-bipyridine (**4d**)*

Experimental procedure as for **4a**. Yield: white powder (0.262 g, 93%). R_f = 0.3 (CCM, SiO_2, hexane/CH_2Cl_2, 50/50, v/v). ^{1}H NMR (200.1 MHz, $CDCl_3$, 25°C): δ = 8.79 ppm (d, ^5J (H,H) = 1.2 Hz, 1H), 8.68 (m, 1H), 8.41 (m, 2H), 7.90 (dd, ^3J (H,H) = 8.2 Hz, ^4J (H,H) = 2.1 Hz, 1H), 7.80 (ddd, ^3J (H,H) = 7.8 Hz, ^4J (H,H) = 1.8 Hz, 1H), 7.29 (m, 1H), 7.18 (AB system, J (AB) = 8.9 Hz, $\Delta\nu$ = 122.4 Hz, 4H), 3.95 (t, ^3J (H,H) = 6.6 Hz, 2H, OCH_2), 1.78 (m, 2H, CH_2), 1.27 (br, 18H), 0.89 (t, ^3J (H,H) = 6.3 Hz, 3H, CH_3). ^{13}C {^{1}H} NMR (50.3 MHz, $CDCl_3$, 25°C): δ = 159.55, 155.43, 154.29, 151.35, 149.15, 139.00, 136.80, 133.12, 120.66, 120.18, 114.53, 114.27 (C-aromatics), 93.76 (C≡C), 85.01 (C≡C), 68.00 (OCH_2), 31.83 (CH_2), 29.59 (CH_2), 29.52 (CH_2), 29.08 (CH_2), 25.92 (CH_2), 22.61 (CH_2), 14.05 (CH_3). FTIR (KBr, ν/cm^{-1}): 2920 (s), 2851 (m), 2210 (w, $\nu_{C\equiv C}$), 1602 (m), 1576 (w), 1539 (w), 1511 (m), 1463 (m), 1380 (w), 1291 (m), 1252 (s), 1108 (s), 1024 (w), 832 (w). FAB$^+$-MS (*m*-NBA): $[M + H]^+$ (% rel. int.): 440.7 (100). Elemental analysis, calc. (found) for $C_{30}H_{36}N_2O$ (M_r = 440.634): C 81.78 (81.55), H 8.24 (8.09), N 6.36 (6.20)%.

5.5. *5-(4-Tetradecyloxyphenylethynyl)-2,2′-bipyridine (**4e**)*

Experimental procedure as for **4a**. Yield: white powder (0.262 g, 93%). R_f = 0.3 (CCM, SiO_2, hexane/CH_2Cl_2, 50/50, v/v). ^{1}H NMR (200.1 MHz, $CDCl_3$, 25°C): δ = 8.79 ppm (dd, ^4J (H,H) = 2.1 Hz, ^5J (H,H) = 0.8 Hz, 1H), 8.69 (m, 1H), 8.41 (m, 2H), 7.91 (dd, ^3J (H,H) = 8.3 Hz, ^4J (H,H) = 2.1 Hz, 1H), 7.83 (dd, ^3J (H,H) = 7.7 Hz, ^4J (H,H) = 1.7 Hz, 1H), 7.32 (m, 1H), 7.19 (AB system, J (AB) = 8.9 Hz, $\Delta\nu$ = 120.7 Hz, 4H), 3.98 (t, ^3J (H,H) = 6.5 Hz, 2H, OCH_2), 1.78 (m, 2H, CH_2), 1.27 (br, 22H), 0.88 (t, ^3J (H,H) = 6.5 Hz, 3H, CH_3). ^{13}C {^{1}H} NMR (50.3 MHz, $CDCl_3$, 25°C): δ = 159.55, 155.47, 154.29, 151.35, 149.15, 139.00, 136.80, 133.12, 121.18, 120.66, 120.18, 114.53, 114.27 (C-aromatics), 93.76 (C≡C), 85.01 (C≡C), 68.00 (OCH_2), 31.87 (CH_2), 29.59 (CH_2), 29.52 (CH_2), 29.30 (CH_2), 29.11 (CH_2), 25.92 (CH_2), 22.65 (CH_2), 14.08 (CH_3). FTIR (KBr, ν/cm^{-1}): 2923 (s), 2852 (m), 2212 (w, $\nu_{C\equiv C}$), 1603 (m), 1575 (w), 1539 (w), 1511 (m), 1464 (m), 1383 (w), 1290 (m), 1248 (s), 1109 (s), 1029 (m), 831 (w). FAB$^+$-MS (*m*-NBA): $[M + H]^+$ (% rel. int.): 469.3 (100). Elemental analysis, calc. (found) for $C_{32}H_{40}N_2O$ (M_r = 468.688): C 82.01 (81.91), H 8.60 (8.51), N 5.98 (5.81)%.

5.6. *5-(4-Hexadecyloxyphenylethynyl)-2,2′-bipyridine (**4f**)*

Experimental procedure as for **4a**. Yield white powder (0.30 g, 94%). ^{1}H NMR (200.1 MHz, $CDCl_3$, 25°C): δ = 8.79 ppm (dd, ^4J (H,H) = 2.4 Hz, ^5J (H,H) = 0.9 Hz, 1H), 8.68 (m, 1H), 8.40 (m, 2H), 7.90 (dd, ^3J (H,H) = 8.2 Hz, ^4J (H,H) = 2.1 Hz, 1H), 7.81 (ddd, ^3J (H,H) = 7.8 Hz, ^4J (H,H) = 1.8 Hz, 1H), 7.30 (m, 1H), 7.19 (AB system, J (AB) = 8.9 Hz, $\Delta\nu$ = 121.8 Hz, 4H), 3.96 (t, ^3J (H,H) = 6.6 Hz, 2H, OCH_2), 1.79 (m, 2H, CH_2), 1.27 (br, 26H), 0.88 (t, ^3J (H,H) = 6.4 Hz, 3H, CH_3). ^{13}C {^{1}H} NMR (50.3 MHz, $CDCl_3$, 25°C): δ = 159.55, 155.47, 154.29, 151.94, 151.35, 149.15, 139.00, 136.83, 133.12, 123.71, 121.18, 120.18, 114.53, 114.27 (C-aromatics), 93.72 (C≡C), 85.01 (C≡C), 68.00 (OCH_2), 31.87 (CH_2), 29.52 (CH_2), 29.30 (CH_2), 29.08 (CH_2), 25.92 (CH_2), 22.61 (CH_2), 14.04 (CH_2). FTIR (KBr, ν/cm^{-1}): 2920 (s), 2851 (s), 2216 (w, $\nu_{C\equiv C}$), 1600 (m), 1578 (w), 1542 (w), 1511 (m), 1466 (m), 1384 (w), 1288 (m), 1251 (s), 1288 (w), 1109 (m), 1024 (m), 931 (w), 832 (w). FAB$^+$-MS (*m*-NBA): [M + H]$^+$ (% rel. int.): 497.3 (100). Elemental analysis, calc. for $C_{34}H_{44}N_2O$ (M_r = 496.743): C 82.21 (82.09), H 8.93 (8.74), N 5.64 (5.46)%.

5.7. *5-Bromo-5′-(4-hexyloxyphenylethynyl)-2,2′-bipyridine (**5a**)*

5,5′-Dibromo-2,2′-bipyridine (0.776 g; 2.47 mmol), 1-ethynyl-4-hexyloxybenzene (**2a**) (0.50 g, 2.47 mmol), and [Pd(PPh_3)$_4$] (0.029 g; 1 mol %) were dissolved in argon-degassed di-isopropylamine (40 ml). The suspension was heated at 60°C for 3 days. After evaporation of the solvent, the residue was purified by flash chromatography (NEt_3 treated silica gel column, elution in a gradient of hexane/CH_2Cl_2: 95/5 to 50/50 v/v) and recrystallized from CH_2Cl_2/hexane. Yield: white powder (0.34 g, 32%). R_f = 0.7 (CCM, SiO_2/NEt_3, hexane/CH_2Cl_2, 95/5, v/v). ^{1}H NMR (200.1 MHz, $CDCl_3$, 25°C): δ = 8.77 ppm (d, ^4J (H,H) = 2.0 Hz, 1H), 8.71 (d, ^4J (H,H) = 2.0 Hz, 1H), 8.34 (m, 2H), 7.92 (ddd, ^3J (H,H) = 8.5 Hz, ^4J (H,H) = 2.1 Hz, 2H), 7.19 (AB system, J (AB) = 8.9 Hz, $\Delta\nu$ = 120.3 Hz, 4H), 3.99 (t, ^3J (H,H) = 6.6 Hz, 2H, OCH_2), 1.80 (m, 2H, CH_2), 1.37 (m, 6H), 0.91 (t, ^3J (H,H) = 6.4 Hz, 3H, CH_3). ^{13}C {^{1}H} NMR (50.3 MHz, $CDCl_3$, 25°C): δ = 159.52, 154.05, 153.40, 151.44, 150.17, 139.42, 139.04, 133.13, 122.42, 121.15, 121.00, 120.11, 114.56, 114.19 (C-aromatics), 94.06 (C≡C), 84.94 (C≡C), 68.04 (OCH_2), 31.49 (CH_2), 29.06 (CH_2), 25.63 (CH_2), 22.51 (CH_2), 14.00 (CH_3). FTIR (KBr, ν/cm^{-1}): 2929 (s), 2863 (m), 2210 (w, $\nu_{C\equiv C}$), 1602 (m), 1537 (w), 1507 (s), 1450 (s), 1389 (w), 1357 (w), 1285 (m), 1248 (s), 1111 (s), 1017 (w), 836 (s). FAB$^+$-MS (*m*-NBA): [M + H]$^+$ (% rel. int.): 437.1/439.1 (32). Elemental analysis, calc. (found) for $C_{24}H_{23}BrN_2O$ (M_r = 435.368): C 66.21 (66.15), H 5.32 (5.28), N 6.43 (6.37)%.

5.8. *5-Bromo-5′-(4-octyloxyphenylethynyl)-2,2′-bipyridine (**5b**)*

Experimental procedure as for **5a**. Yield: white solid (0.30 g, 33%). R_f = 0.7 (CCM, SiO_2/NEt_3, hexane/CH_2Cl_2, 95/5, v/v). ^{1}H NMR (200.1 MHz, $CDCl_3$, 25°C): δ = 8.77 ppm (dd, ^4J (H,H) = 2.0 Hz, ^5J (H,H) = 0.7 Hz, 1H), 8.72 ppm (dd, ^4J (H,H) = 2.1 Hz, ^5J (H,H) = 0.7 Hz, 1H), 8.34 (m, 2H), 7.92 (ddd, ^3J (H,H) = 8.2 Hz, ^4J (H,H) = 2.1 Hz, 2H), 7.19 (AB system, J (AB) = 8.9 Hz, $\Delta\nu$ = 120.5 Hz, 4H), 3.98 (t, ^3J (H,H) = 6.6 Hz, 2H, OCH_2), 1.80 (m, 2H, CH_2), 1.30 (br, 10H), 0.89 (t, ^3J (H,H) = 6.8 Hz, 3H, CH_3). ^{13}C {^{1}H} NMR (50.3 MHz, $CDCl_3$, 25°C): δ = 159.70, 154.04, 153.37, 151.48, 150.23, 139.47, 139.12, 133.21, 122.49, 121.21, 121.08, 120.18, 114.62, 114.25 (C-aromatics), 94.13 (C≡C), 84.99 (C≡C), 68.10 (OCH_2), 31.77 (CH_2), 29.31 (CH_2), 29.19 (CH_2), 29.15 (CH_2), 25.98 (CH_2), 22.63 (CH_2), 14.10 (CH_3). FTIR (KBr, ν/cm^{-1}): 2925 (s), 2857 (m), 2214 (w, $\nu_{C\equiv C}$), 1602 (m), 1537 (w), 1506 (s), 1453 (s), 1389 (w), 1285 (m), 1250 (s), 1112 (s), 999 (m), 836 (m). FAB$^+$-MS (*m*-NBA): [M + H]$^+$ (% rel. int.): 463.1/465.1 (100). Elemental analysis, calc. (found) for $C_{26}H_{27}BrN_2O$ (M_r = 463.422): C 67.39 (67.22), H 5.87 (5.64), N 6.04 (5.82)%.

5.9. *5-Bromo-5′-(4-decyloxyphenylethynyl)-2,2′-bipyridine (**5c**)*

Experimental procedure as for **5a**. Yield: white solid (0.32 g, 34%). R_f = 0.7 (CCM, SiO_2/NEt_3, hexane/CH_2Cl_2, 95/5, v/v). ^{1}H NMR (200.1 MHz, $CDCl_3$, 25°C): δ = 8.74 ppm (dd, ^3J (H,H) = 8.7 Hz, ^4J (H,H) = 2.0 Hz, 2H), 8.34 (m, 2H), 7.92 (ddd, ^3J (H,H) = 8.5 Hz, ^4J (H,H) = 2.1 Hz, 2H), 7.19 (AB system, J (AB) = 8.9 Hz, $\Delta\nu$ = 120.3 Hz, 4H), 3.98 (t, ^3J (H,H) = 6.6 Hz, 2H, OCH_2), 1.80 (m, 2H, CH_2), 1.28 (br, 14H), 0.89 (t, ^3J (H,H) = 6.4 Hz, 3H, CH_3). ^{13}C {^{1}H} NMR (50.3 MHz, $CDCl_3$, 25°C): δ = 159.61, 154.15, 153.48, 151.58, 150.35, 139.57, 139.22, 133.32, 122.60, 121.32, 121.19, 120.29, 114.74, 114.38 (C-aromatics), 94.25 (C≡C), 85.12 (C≡C), 68.22 (OCH_2), 31.99 (CH_2), 29.66 (CH_2), 29.48 (CH_2), 29.27 (CH_2), 26.11 (CH_2), 22.78 (CH_2), 14.22 (CH_3). FT-IR (KBr, ν/cm^{-1}): 2923 (s), 2853 (m), 2212 (w, $\nu_{C\equiv C}$), 1605 (m), 1574 (w), 1537 (w), 1510 (s), 1454 (s), 1359 (w), 1286 (m), 1251 (s), 1102 (s), 1016 (m), 836 (s). FAB$^+$-MS (*m*-NBA): [M + H]$^+$ (% rel. int.): 493.1/495.1 (100). Elemental analysis, calc. (found) for $C_{28}H_{31}BrN_2O$ (M_r = 491.476): C 68.43 (68.11), H 6.36 (6.13), N 5.70 (5.55)%.

5.10. *5-Bromo-5′-(4-dodecyloxyphenylethynyl)-2,2′-bipyridine (**5d**)*

Experimental procedure as for **5a**. Yield: white powder (0.40 g, 44%). R_f = 0.7 (CCM, SiO_2/NEt_3, hexane/CH_2Cl_2, 95/5, v/v). ^{1}H NMR (200.1 MHz, $CDCl_3$, 25°C):

δ = 8.76 ppm (dd, ^4J (H,H) = 2.1 Hz, ^5J (H,H) = 0.7 Hz, 1H), 8.72 (d, ^4J (H,H) = 2.1 Hz, 1H), 8.35 (m, 2H), 7.92 (ddd, ^3J (H,H) = 8.5 Hz, ^4J (H,H) = 2.4 Hz, 2H), 7.19 (AB system, J (AB) = 8.9 Hz, $\Delta\nu$ = 120.3 Hz, 4H), 3.98 (t, ^3J (H,H) = 6.6 Hz, 2H, OCH_2), 1.80 (m, 2H, CH_2), 1.27 (br, 18H), 0.88 (t, ^3J (H,H) = 6.4 Hz, 3H, CH_3). ^{13}C {^1H} NMR (50.3 MHz, $CDCl_3$, 25°C): δ = 159.82, 154.17, 153.51, 151.60, 150.37, 139.60, 139.25, 133.32, 122.61, 121.33, 121.19, 120.31, 114.75, 114.37 (C-aromatics), 94.24 (C≡C), 85.10 (C≡C), 68.23 (OCH_2), 32.00 (CH_2), 29.67 (CH_2), 29.45 (CH_2), 29.26 (CH_2), 26.09 (CH_2), 22.78 (CH_2), 14.20 (CH_3). FTIR (KBr, ν/cm^{-1}): 2921 (s), 2852 (m), 2213 (w, $\nu_{C\equiv C}$), 1603 (m), 1537 (w), 1511 (m), 1452 (s), 1390 (w), 1289 (w), 1252 (m), 1102 (s), 1109 (s), 1013 (w), 836 (m). FAB$^+$-MS (*m*-NBA): [M + H]$^+$ (% rel. int.): 519.9/521.1 (35). Elemental analysis, calc. (found) for $C_{30}H_{35}BrN_2O$ (M_r = 519.530): C 69.36 (69.27), H 6.79 (6.68), N 5.39 (5.24)%.

5.11. *5-Bromo-5′-(4-tetradecyloxyphenylethyny l)-2,2′-bipyridine (**5e**)*

Experimental procedure as for **5a**. Yield: white powder (0.35 g, 40%). R_f = 0.7 (CCM, SiO_2/NEt_3, hexane/CH_2Cl_2, 95/5, v/v). ^1H NMR (200.1 MHz, $CDCl_3$, 25°C): δ = 8.76 ppm (dd, ^4J (H,H) = 2.0 Hz, ^5J (H,H) = 0.9 Hz, 1H), 8.72 (dd, ^4J (H,H) = 2.5 Hz, ^5J (H,H) = 0.7 Hz, 1H), 8.35 (m, 2H), 7.92 (ddd, ^3J (H,H) = 8.3 Hz, ^4J (H,H) = 2.1 Hz, 2H), 7.19 (AB system, J (AB) = 8.9 Hz, $\Delta\nu$ = 120.3 Hz, 4H), 3.98 (t, ^3J (H,H) = 6.4 Hz, 2H, OCH_2), 1.80 (m, 2H, CH_2), 1.27 (br, 22H), 0.88 (t, ^3J (H,H) = 6.4 Hz, 3H, CH_3). ^{13}C {^1H} NMR (50.3 MHz, $CDCl_3$, 25°C): δ = 159.83, 154.17, 151.60, 150.36, 139.60, 139.25, 133.32, 122.61, 121.33, 120.31, 114.75, 114.37 (C-aromatics), 94.24 (C≡C), 85.09 (C≡C), 68.23 (OCH_2), 32.01 (CH_2), 29.75 (CH_2), 29.46 (CH_2), 29.26 (CH_2), 26.10 (CH_2), 22.78 (CH_2), 14.20 (CH_3). FTIR (KBr, ν/cm^{-1}): 2920 (s), 2851 (m), 2214 (w, $\nu_{C\equiv C}$), 1606 (m), 1537 (w), 1512 (m), 1461 (m), 1390 (w), 1289 (w), 1252 (m), 1104 (s), 1013 (w), 837 (m). FAB$^+$-MS (*m*-NBA): [M + H]$^+$ (% rel. int.): 547.3/549.3 (100). Elemental analysis, calc. (found) for $C_{32}H_{39}BrN_2O$ (M_r = 547.584): C 70.19 (69.81), H 7.18 (6.98), N 5.12 (4.84)%.

5.12. *5-Bromo-5′-(4-hexadecyloxyphenylethyny l)-2,2′-bipyridine (**5f**)*

Experimental procedure as for **5a**. Yield: white powder (0.28 g, 30%). R_f = 0.7 (CCM, SiO_2/NEt_3, hexane/CH_2Cl_2, 95/5, v/v). ^1H NMR (200.1 MHz, $CDCl_3$, 25°C): δ = 8.77 ppm (dd, ^4J (H,H) = 2.1 Hz, ^5J (H,H) = 0.7 Hz, 1H), 8.72 (dd, ^4J (H,H) = 2.5 Hz, 1H), 8.34 (m, 2H), 7.92 (ddd, ^3J (H,H) = 8.5 Hz, ^4J (H,H) = 2.1 Hz, 2H), 7.19 (AB system, J (AB) = 8.9 Hz, $\Delta\nu$ = 120.3 Hz, 4H), 3.98 (t, ^3J (H,H) = 6.6 Hz, 2H, OCH_2), 1.79 (m, 2H, CH_2), 1.26 (br, 26H), 0.88 (t, ^3J (H,H) = 6.4 Hz, 3H, CH_3). ^{13}C {^1H} NMR (50.3 MHz, $CDCl_3$, 25°C): δ = 159.83, 154.18, 153.53, 151.60, 150.37, 139.60, 139.25, 133.32, 122.61, 121.33, 120.31, 114.75, 114.37 (C-aromatics), 94.23 (C≡C), 85.09 (C≡C), 68.24 (OCH_2), 32.01 (CH_2), 29.76 (CH_2), 29.66 (CH_2), 29.45 (CH_2), 29.26 (CH_2), 26.09 (CH_2), 22.77 (CH_2), 14.20 (CH_3). FTIR (KBr, ν/cm^{-1}): 2919 (s), 28501 (m), 2214 (w, $\nu_{C\equiv C}$), 1606 (m), 1512 (m), 1464 (m), 1390 (w), 1288 (w), 1252 (m), 1108 (s), 1016 (w), 837 (m). FAB$^+$-MS (*m*-NBA): [M + H]$^+$ (% rel. int.): 575.6/577.2 (100). Elemental analysis, calc. (found) for $C_{34}H_{43}BrN_2O$ (M_r = 575.639): C 70.94 (70.64), H 7.53 (7.21), N 4.87 (4.65)%.

The present work was supported by the Centre National de la Recherche Scientifique (CNRS) and by the Strasbourg School of Chemical Engineering (ECPM).

References

[1] (*a*) Constable, E. C., 1989, *Adv. Inorg. Chem.*, **34,** 1 and references therein; (*b*) Lehn, J. M., 1995, *Supramolecular Chemistry* (New York: VCH).

[2] Kraft, A., Grimsdale, A. C., and Holmes, A. B., 1998, *Angew. Chem. int. Ed. Engl.*, **37,** 402.

[3] Leclerc, M., 1999, *Adv. Mater.*, **11,** 1491.

[4] (*a*) Giroud-Godquin, A. M., and Maitlis, P. M., 1991, *Angew. Chem. int. Ed. Engl.*, **30,** 375; (*b*) Espinet, P., Esteruela, M. A., Oro, L. A., Serrano, J. L., and Sola, E., 1992, *Coord. Chem. Rev.*, **117,** 215; (*c*) Bruce, D. W., 1993, *Inorganic Materials*, edited by D. W. Bruce and D. O'Hare (Chichester: Wiley); (*d*) Serrano, L., and Sierra, T., 1996, in *Metallomesogens*, edited by L. Serrano (Weinheim: VCH), pp. 107–111.

[5] (*a*) Bruce, D. W., and Rowe, K. E., 1995, *Liq. Cryst.*, **18,** 161; (*b*) Bruce, D. W., and Rowe, K. E., 1996, *Liq. Cryst.*, **20,** 183; (*c*) Bruce, D. W., and Rowe, K. E., 1995, *J. Chem. Soc. Dalton Trans.*, 3913; (*d*) Douce, L., Ziessel, R., Seghrouchni, R., Skoulios, A., Campillos, E., and Deschenaux, R., 1995, *Liq. Cryst.*, **18,** 157.

[6] El-Ghayoury, A., Douce, L., Ziessel, R., and Skoulios, A., 1998, *Angew. Chem. Int. Ed. Engl.*, **37,** 1235.

[7] (*a*) El-Ghayoury, A., Douce, L., Ziessel, R., and Skoulios, A., 1998, *Angew. Chem. int. Ed. Engl.*, **37,** 2205; (*b*) Ziessel, R., Douce, L., El-Ghayoury, A., Harriman, A., and Skoulios, A., 2000, *Angew. Chem. Int. Ed. Engl.*, **39,** 1549.

[8] (*a*) Douce, L., Ziessel, R., Seghrouchni, R., and Skoulios, A., 1996, *Liq. Cryst.*, **21,** 143; (*b*) Douce, L., Ziessel, R., Hsuan-Hong, L., and Hong-Cheu, L., 1999, *Liq. Cryst.*, **26,** 1797.

[9] Leininger, S., Olenyuk, B., and Stang, P. J., 2000, *Chem. Rev.*, **100,** 853.

[10] Romero, F. M., and Ziessel, R., 1995, *Tetrahedron Lett.*, **36,** 6471.
[11] Synthesis adapted from Masahiro, S., Kunikyo, Y., and Hiroshi, H., Japanese Pat. Tokyo, KOHO JP01 56,624[89 56,624] and *Chem. Abs.*, **111**: 164755m.
[12] Guillon, D., Skoulios, A., and Benattar, J. J., 1986, *J. Phys., Paris*, **47,** 133.
[13] (*a*) Tsiourvas, D., Paleos, C. M., and Skoulios, A., 1999, *Macromolecules*, **32,** 8059; (*b*) Alami, E., Levy, H., Zana, R., Weber, P., and Skoulios, A., 1993, *Liq. Cryst.*, **13,** 201; (*c*) Guillon, D., and Skoulios, A., 1984, *J. Phys., Paris*, **45,** 607.
[14] (*a*) Pershan, P. S., 1988, *Structure of Liquid Crystal Phases* (Singapore: World Scientific Publishing); Chandrasekhar, S., 1992, *Liquid Crystals*, 2nd Ed., (Cambridge University Press); (*b*) De Gennes, P. G., and Prost, J., 1993, *The Physics of Liquid Crystals* (Oxford: Clarendon Press).
[15] Pindak, R., Moncton, D. E., and Davey, S. C., 1981, *Phys. Rev. Lett.*, **46,** 1135.